A Closed-Loop Ear Wearable EEG Measurement Device with Realtime Electrode Skin Impedance Measurement

Muhammad Sheeraz[1], Abdul Rehman Aslam[1], Muhammad Awais Bin Altaf[1], and Hadi Heidari[2]
Lahore University of Management Sciences[1], Pakistan. University of Glasgow[2], United Kingdom.
Email: {muhammad.sheeraz, 17060056, awais.altaf}@lums.edu.pk; hadi.heidari@glasgow.ac.uk

***Abstract*—Electroencephalogram (EEG) play a vital role in the prediction of neurological disorders including epilepsy, narcolepsy, migraine, etc. The impedance between the electrodes and the skin interface should be within specific range in order to acquire good quality EEG signals. This work focuses on an intelligent, wearable device capable of measuring electrode-skin interface impedance (ESI) in parallel to the EEG acquisition in non-invasive manner. The proposed device includes an analog front end (AFE), back-end micro-controller (BEM), and ESI measuring unit. A novel technique is used for measurement of ESI by connecting known value resistances in parallel at the input terminals of the low noise amplifier (LNA) of AFE and measuring the change in the output signal. This unique technique is suitable in wearable medical devices as it is safe to use, results in high-quality EEG signals, and consumes negligible power. A PCB prototype is developed using the available commercial components. The designed prototype has a small form factor (52mm x 53mm), is lightweight, and easily behind the ear wearable.**

***Index Terms*—Electroencephalogram (EEG), Electrode-Skin Interface Impedance (ESI), Analog Front End (AFE), Back-End Micro-controller (BEM), Low Noise Amplifier (LNA).**

I. Introduction

Physiological signals including electroencephalogram (EEG) or electrocardiogram (ECG) are measured using high-grade medical equipment in clinical settings. These high-grade medical devices are non-portable, bulky, and require initialization procedures [1]. The patients have to sit or lay down in a certain position during the whole measurement. A trained technician is also required to operate these devices [1]. The primary issue with these devices is their availability in specialized healthcare centers only, which are not accessible to everyone. A large population of people is deprived of specialized healthcare facilities worldwide, due to which many serious health issues remain undiagnosed at an early stage [2] - [6].

EEG signals play a vital role in the detection of neurological disorders like epileptic seizures, autism spectrum disorder, Parkinson's disease, etc [7]. Current ambulatory EEG measuring devices impose restrictions on the patients for performing daily life activities and are hence not suitable for longer duration measurements [8], [9]. To diagnose and treat neurological disorders continuous recording of brain signals for a longer duration is required [10]- [12].

Continuous monitoring EEG devices can aid the earlier detection of many health problems and avoid serious health issues [8], [9]. The primary challenges in this regard are the form factor and signal-to-noise ratio (SNR) of bio-signal acquisition devices. Major noise sources include external power lines interface, artifacts, and electrode skin interface impedance (ESI) [13]. ESI is one of the major sources for the quality degradation of bio-signals. Large ESI leads to the low noise amplifier (LNA) saturation, common-mode rejection ratio (CMRR) reduction and the system's susceptibility to external noises increase [14].

Pre-gelled or metal disc electrodes are usually used for skin contact. Different factors including pressure, size, type, and usage duration of the electrodes impact ESI. The equivalent circuit model defined by Webster is depicted in Fig. 1 [17]. E_{HC} is the half-cell potential of the electrode, R_D, and C_D are the electrode-electrolyte interface resistance and capacitance, respectively. R_G is the resistance of the gel, E_E is the potential between the epidermis and the gel. R_E and C_E are the resistance and capacitance of the epidermis, respectively. R_S is the resistance of the subcutaneous tissues of the skin.

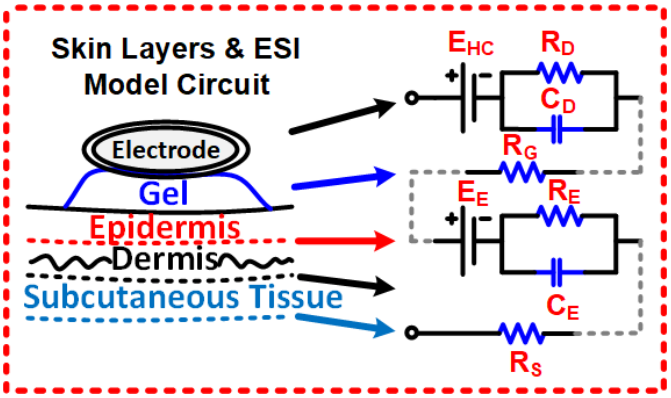

Fig. 1. Skin Layers and Equivalent Webster ESI Model

Conventionally, the ESI is measured by injecting a known square wave current source and measuring the differential voltage across electrodes [18]. The current injection method consumes power for injecting current into the system and hence the backup time of portable devices decreases significantly. It is also dangerous as it can cause shocks to the patient

and may result in abrasions on the skin. [14].

This paper targets a novel, single-channel, behind-the-ear wearable EEG acquisition device using pre-gelled Ag/AgCl electrodes in a non-invasive manner [8], [15]. The proposed device is capable of measuring the ESI intelligently in a closed-loop manner during the EEG acquisition [16]. The system also provides feedback to the user regarding the proper placement of electrodes and ESI values. To avoid the saturation of the AFE, Programmable Gain Amplifier (PGA) control is available for achieving better results via controlling the overall gain of the system. The prototype doesn't impose any restrictions on the user as it is of small form factor and transmits data wirelessly. The proposed device makes sure to obtain better quality EEG signals by limiting the unwanted effects caused due to ESI, improper electrodes placement, and other parameters that degrades the quality of the physiological signals [16].

II. Proposed System

The American Clinical Neurophysiology Society (ACNS) has set guidelines for recording clinical EEG on digital media [19] and long-term monitoring for epilepsy [20]. Table I summarizes the ACNS guidelines for the EEG measurement. The sampling rate limits, digitization resolution, dynamic range, CMRR, noise level, low-frequency response, high-frequency response, and input impedance are listed in Table I. Our proposed device is according to these ACNS standards.

TABLE I
American Clinical Neurophysiology Society Guidelines

ACNS Guidelines [19] [20]	
Device Parameters	**Recommended Value**
Sampling Rate	$\geq$256 Samples per second
Digitization Resolution	$\geq$16 Bit
Dynamic Range	$>$40dB
CMRR	$\geq$60dB
Noise Level	$\leq 1\mu$V
Low Frequency Response	0.5Hz or lower
High Frequency Response	70Hz or higher
Input Impedance	>1MΩ

The proposed EEG measuring system consists of three main parts including AFE, back end microcontroller (BEM), and ESI measuring unit. AFE acquires the EEG signals, amplifies, removes noise, artifacts, and offsets in the measured EEG signals. BEM receives the measured analog EEG signals from AFE and converts them to digital form using built-in ADC and finally transmit the digitized EEG data to the mobile phone wirelessly via BLE. BEM also controls the switching of the ESI unit and performs all the required calculations for impedance measuring unit. ESI unit consists of known value resistors that are connected to the input of the LNA via switches for measuring the ESI. Fig. 2 shows the overall block diagram of the proposed system.

A. Analog Front End (AFE)

The AFE acquires the analog EEG signals, amplifies and pre-process the acquired EEG. It includes the LNA, an anti-aliasing filter (AAF), and the PGA. INA333 is used as LNA which provides the CMRR $>$100dB, input impedance >1GΩ

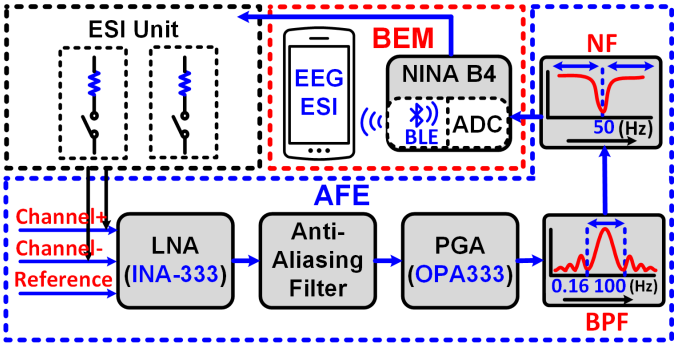

Fig. 2. Overall System Block Diagram.

and noise of about 650nV$_{rms}$ for the band of 0.16Hz-100Hz. All the AFE parameters are according to the ACNS guideline mentioned in Table 1. Fig. 3 shows the electrodes placement and AFE schematics along with the ESI unit.

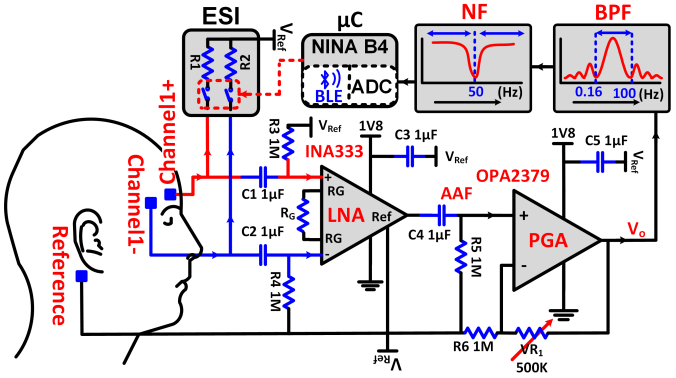

Fig. 3. Electrodes Placement and AFE Schematics

A differential EEG channel is connected to the LNA input, which significantly reduced the artifacts and power line interference. The INA333 amplifier gain was set at 15 times in order to avoid LNA saturation. An AAF with a cut-off frequency of 0.16 Hz is present after LNA for the removal of electrodes DC offset [22]. This offset voltage is induced when an electrode is placed on the skin and depends upon the electrode type, electrolyte composition, and body temperature [21]. The PGA further amplifies the received EEG signals. OPA2379 in non-inverting configuration is used as PGA with a variable gain. A BPF having a lower and upper cut-off frequency of 0.16 Hz and 100 Hz, respectively is added after PGA to get the desired band EEG signal. It filters out the unwanted frequency components and removes the DC offset and motion artifacts from the acquired EEG signal [21] A 50 Hz notch filter (NF) is cascaded after the BPF to remove the 50Hz frequency component due to power lines interference.

B. Back-End Microcontroller (BEM)

NINA-B316 bluetooth low energy (BLE) module by u-blox is used as the BEM unit. It is an ultra-low-power microcontroller with a built-in BLE transceiver. The analog EEG signal acquired from the AFE is transferred to the SAR-ADC

of NINA-B316. The 14-bit SAR-ADC digitizes the EEG signal with a sampling rate of 256 samples per second. The digitized EEG signal stored in μC is transmitted to the mobile phone via BLE and is also stored on the web-server. NINA-B316 manages the EEG data storage, transmission, and switching for the ESI measurement. It also performs the calculations related to the ESI classification. Fig.2 shows the BEM unit embedded in the proposed EEG acquisition device.

C. Electrode-Skin Interface Impedance (ESI) Measuring Unit

A novel passive technique is applied for the measurement of ESI. No external active known current is injected into the system. The voltage level of physiological signal itself is measured for the calculation of the ESI. Fig. 4 shows the complete ESI hardware configuration details. It basically consists of known value (5.6kΩ, 0.1%) resistors R1 and R2 at the input terminals of the LNA. These resistors are connected via IC MAX4741EUA+ switches which are controlled by BEM. AAF is added at both the input terminals of the LNA to remove the DC offset of electrodes [22]. In order to measure the ESI, these resistors are connected in parallel at the input terminals (In+ & In-) of LNA, and the variation in the voltage level of output signal is measured. The output signal is measured during two configurations i.e. before and after connecting the resistors R1 & R2, respectively. Measured signals are stored in the BEM. BEM calculates the root mean square voltage (V_{rms}) and performs the calculation for determining the approximate value of the ESI.

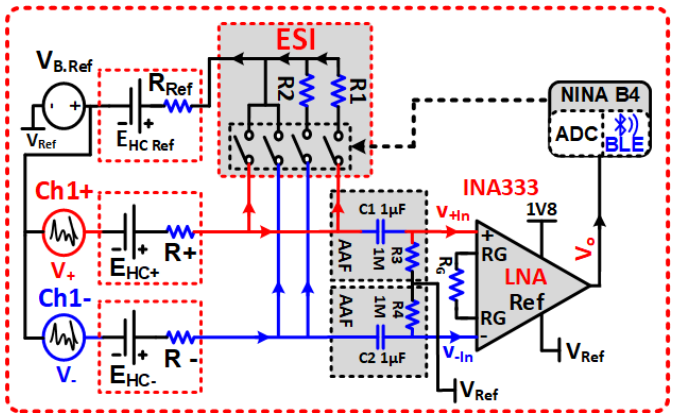

Fig. 4. ESI Measuring Model and Schematics

The assumed ESI model along with complete schematic related to ESI measuring unit is shown in Fig. 4. Webster model [17] is being used for modeling the ESI as indicated in Fig. 1. We have neglected R_S, R_E & R_G as these resistances are so small compared to the ESI [24]. EEG bio-signal itself is measured for the calculation of ESI, hence for our specified frequency band of 0.16Hz–100Hz reactance of the capacitors is assumed to be frequency independent and is already incorporated in the equivalent resistance R_+ & R_- of $Ch1_+$ & $Ch1_-$ electrodes, respectively. After these assumptions, the equivalent Webster model for ESI becomes a voltage source with a series resistance as shown in Fig. 4. V_+ and V_- is the voltage amplitude of EEG signal from the brain at $Ch1_+$ & $Ch1_-$ electrodes, respectively. The electrode offset voltage is shown by battery E_{HC+} and E_{HC-} for the positive and negative channel electrodes, respectively. Known value parallel resistors, connected for the measurement of ESI are represented by R1 and R2. The Eq. 1 provides the voltage V_{+In} at the positive input terminal of LNA when In_+ of LNA is in normal mode (R_1 is not connected). Eq. 2 provides the voltage V_{+In} at the positive input terminal of LNA when parallel resistor $R1$ is connected to the positive terminal of LNA. Eq. 3 provides the measured ESI. Similarly, these equations are also applicable to the negative channel. All the processing and calculations for measuring the ESI are performed by BEM.

$$V_{+In} = V_+ \times \frac{R_3}{R_3 + X_{C1} + R_+} \tag{1}$$

$$V_{+In} = \frac{R_3}{R_3 + X_{C1}} \times \frac{R_1}{R_1 + R_+} \times V_+ \tag{2}$$

$$R_+ = \frac{R_1 R_3}{R_3 + X_{C1}} \times \frac{V_+}{V_{+In}} - R_1 \tag{3}$$

As pre-gelled Ag/AgCl electrodes are used during the measurement procedure, a threshold of 10kΩ is selected for the impedance status. Impedance value up to 10kΩ is considered to be normal/low impedance as in the literature impedance around 10kΩ is acceptable for the good quality signal acquisition [24]. If the impedance value is above the 10kΩ the BEM will update the user that the impedance is high via an indicator in the mobile phone application. After getting the message on the mobile phone user performs the necessary steps including the system overall gain adjustment via PGA control and checking electrodes placement whether they are properly placed or not.

III. Device Power Profile & Prototype

A rechargeable EEG device with standard type-B micro USB cable is presented. The system is powered up using a 3.7V 700 mAh Li-ion polymer battery. The operating voltage is set at 1.8V in order to reduce the power consumption of the overall system. STLQ020C18R, 1.8V linear voltage regulator with ultra-low quiescent (0.3μA) current is used for providing a constant 1.8V to the system. The reference voltage of 0.9V is provided via a low impedance buffer. The proposed device provides a backup of about 7 days on one full charge.

Fig. 5 shows the designed PCB, assembled device, acquired EEG signal and measured ESI values. The PCB is designed in Altium Designer21 and developed from the PCB fabrication facility. Fig. 5(a) shows the complete PCB board including BEM, PGA gain control, LNA, and PGA units. Fig. 5(b) shows the completely assembled device. The device enclosure is designed in SOLID-WORKS and developed using a 3D printer. The overall dimensions of the prototype are 52mm x 53mm, PGA gain control is provided at the front side of the device. Fig.5(c) depicts the acquired EEG signal on the mobile

phone along with the feedback regarding electrodes placement and ESI measurement.

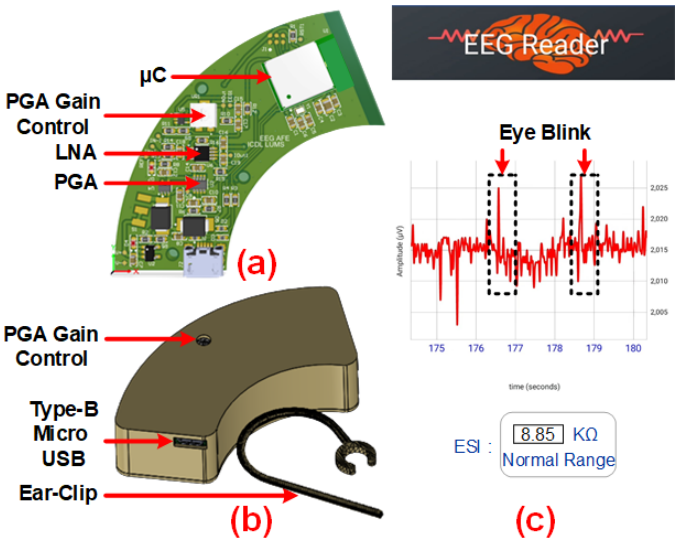

Fig. 5. (a) PCB, (b) Assembled Device and (c) Mobile Application

IV. Measurements and Results

The proposed device is tested and validated using EEG and ESI measurements. The acquired results are compared with the related state-of-the-art works. Table II summarizes the comparison of this work with the other works. This system is the 1st (to the best of our knowledge), wearable behind-the-ear, ultralow-power device capable of acquiring EEG signal along with ESI measurement in line with ACNS Standards [20]. ESI measurement is obtained using a novel passive technique with minimum power consumption and no shocks. The previous works provide the ESI measurement using active current injecting techniques [23], [25] with high risks of shocks or abrasion to skin [23], [25]. Some research works do not provide ESI measurements and only provide EEG measurement [8].

TABLE II

COMPARISON WITH THE STATE-OF-THE-ART-WORKS

Parameters	JOP'16 [25]	EMBC'14 [8]	EMBC'18 [23]	Nature'20 [14]	This Work
Rechargeable	No	No	No	Yes	Yes
Wearable	No	Yes	No	---	Yes
Dimensions (mm^2)	----	60 x 64	----	----	52 x 53
ESI/Technique	Yes/Active	No/----	Yes/Active	Yes/Passive	Yes/Passive
Shocks Risk	Yes	No	Yes	No	No
PGA	No	No	No	No	Yes

A. EEG Measurement

EEG signal is measured during various states including eyes open, eyes close, and eyes blinking for testing our designed device. Fig. 6 shows the EEG measurement during eyes open state with some eyes blinking activity along with Fast Fourier transform (FFT). The FFT analysis clearly indicates that the acquired EEG signal has higher delta (0-4Hz) and beta (13-30 Hz) amplitudes as compared to other remaining EEG bands [26].

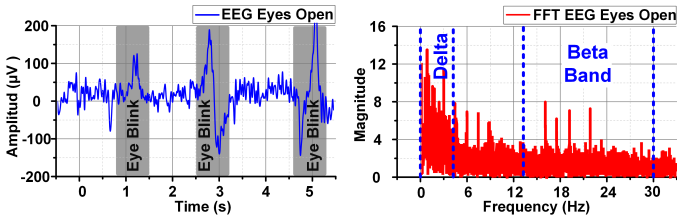

Fig. 6. Measured EEG and its FFT Spectrum

B. ESI Measurement

Multiple ESI measurements with the designed device are obtained using different dry and pre-gelled Ag/AgCl electrodes of variable diameter (8mm - 10mm). Fig. 7 shows the ESI measurements of two different sizes of pre-gelled Ag/AgCl electrodes at various time stamps. Time Stamp # 4 shows the ESI when adequate pressure was applied on the measuring electrodes. It can be observed that the ESI decreases when sufficient pressure is applied [27].

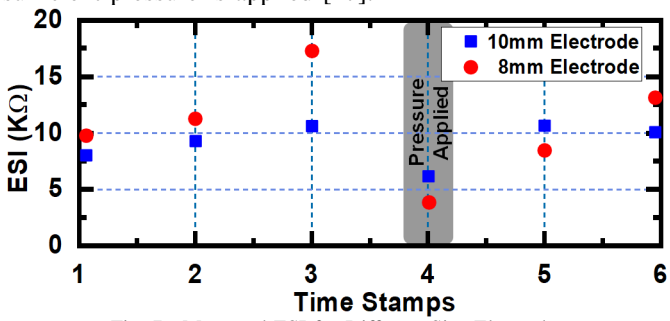

Fig. 7. Measured ESI for Different Size Electrodes

V. Conclusion

In this paper, a novel EEG acquisition device is presented. It imposes no restriction or discomforts to the patients and is easily behind-the -ear wearable. It provides EEG measurement not only for a longer duration but also ensures the quality of the acquired EEG signal by checking the ESI remains at the minimum level. ESI measurement is done using a unique passive energy-efficient and safe technique by connecting known value resistors at the input of LNA. EEG data is stored on to server along with real-time feedback on the mobile phone. This wearable EEG acquisition device is an advancement in the wearable bio-medical devices for better prediction, diagnosis, and treatment of neurological disorders. The proposed device is of small form factor and is capable of working in wireless manner. It provides the real time feed back to the user regarding the EEG signals, electrodes placement and ESI.

Acknowledgment

This work was supported by the National Center of Artificial Intelligence (NCAI), Pakistan Research Fund # RF-NCAI-030 and Syed Babar Ali Research Award, LUMS, Pakistan.

REFERENCES

[1] S. J. Johnstone, R. Blackman and J. M Bruggemann, "EEG from a single-channel dry-sensor recording device." in *Clinical EEG and Neuroscience*, vol. 43, no. 2, pp. 112-120, Mar. 2012.

[2] D. Wu, T. P. Lam, K. F. Lam, K. S. Sun and X. D. Zhou, "Patients' Coping Behaviors to Unavailability of Essential Medicines in Primary Care in Developed Urban China," in *International Journal of Health Policy and Management*, vol. 10, no. 1, pp. 14-21, Jan. 2021.

[3] Z. Taufique, B. Zhu, G. Coppola, M. Shoaran, W. Saadeh and M. A. B. Altaf, "An 8.7 J/class. FFT accelerator and DNN-based configurable SoC for Multi-Class Chronic Neurological Disorder Detection," *IEEE Asian Solid-State Circuits Conference (A-SSCC)*, Nov. 2021, pp. 1-3.

[4] A. Muneeb, M. Ali, and M. A. B. Altaf, "A 2.7μJ/Classification Machine-Learning Based Approximate Computing Seizure Detection SoC," *IEEE International Symposium on Circuits and Systems (ISCAS)*, May 2022, pp. 1-5.

[5] C. Zhang, M. A. B. Altaf and J. Yoo, "A 16-channel, 1-second latency patient-specific seizure onset and termination detection processor with dual detector architecture and digital hysteresis," *IEEE Custom Integrated Circuits Conference (CICC)*, 2015, pp. 1-4.

[6] A. R. Aslam and M. A. B. Altaf, "An 8 Channel Patient Specific Neuromorphic Processor for the Early Screening of Autistic Children through Emotion Detection," *IEEE International Symposium on Circuits and Systems (ISCAS)*, May 2019, pp. 1-5.

[7] A. R. Aslam, N. Hafeez, H. Heidari and M. A. B. Altaf, "An 8.62 μW Processor for Autism Spectrum Disorder Classification using Shallow Neural Network," Proc. *IEEE International Conference on Artificial Intelligence Circuits and Systems (AICAS)*, 2021, pp. 1-4.

[8] B. G. D. Valle, S. S. Cash and C. G. Sodini, "Wireless behind-the-ear EEG recording device with wireless interface to a mobile device (iPhone/iPod touch)." Proc. *IEEE Eng. Med. Bio. Conf. (EMBC)*, Nov. 2014.

[9] F. Pinho, J. J. Cerqueira, J. H. Correia, N. Sousa and N. S. Dias, "myBrain: a novel EEG embedded system for epilepsy monitoring," in *J. of Med. Eng. & Technol.*, vol. 41, no. 7 pp. 564-585, Sep. 2017.

[10] M. Altaf, C. Zhang and J. Yoo, "A 16-Channel Patient-Specific Seizure Onset and Termination Detection SoC With Impedance-Adaptive Transcranial Electrical Stimulator", in *IEEE J. Solid-State Circuits*, vol. 50, no. 11, pp. 2728-2740, Nov. 2015

[11] M. A. B. Altaf and J. Yoo, "A 1.52 uJ/classification patient-specific seizure classification processor using Linear SVM," *IEEE International Symposium on Circuits and Systems (ISCAS)*, May 2013, pp. 849-852.

[12] A. R. Aslam and M. A. B. Altaf, "A 10.13μJ/Classification 2-Channel Deep Neural Network Based SoC for Negative Emotion Outburst Detection of Autistic Children," in *IEEE Transactions on Biomedical Circuits and Systems (TBioCAS)*, vol. 15, no. 5, pp. 1039-1052, Oct. 2021.

[13] M. Guermandi, R. Cardu, E. F. Scarselli and R. Guerrieri, "Active Electrode IC for EEG and Electrical Impedance Tomography With Continuous Monitoring of Contact Impedance," in *IEEE Trans. Biomed. Circuits Syst. (TBioCAS)*, vol. 9, no. 1, pp. 21–33, Feb. 2015.

[14] E. Alonso, R. Giannetti, C. R. Morcillo, J. Matanza and J. D. Muñoz-Frías, "A Novel Passive Method for the Assessment of Skin-Electrode Contact Impedance in Intraoperative Neurophysiological Monitoring Systems." Scientific Reports in *Nature* Feb. 18, 2020.

[15] M. A. B. Altaf and J. Yoo, "A 1.83μJ/Classification, 8-Channel, PatientSpecific Epileptic Seizure Classification SoC Using a Non-Linear Support Vector Machine," in *IEEE Trans. Biomed. Circuits Syst.*, vol. 10, no. 1, pp. 49-60, Feb. 2016

[16] C. H. Chang, S. A. Zahrai, K. Wang, L. Xu, I. Farah, M. Onabajo, "An Analog Front-End Chip With Self-Calibrated Input Impedance for Monitoring of Biosignals via Dry Electrode-Skin Interfaces," in *IEEE Trans. Circuits and Systems*, vol 64, no. 10, pp 2666 - 2678, Oct. 2017.

[17] J. G. Webster, *Medical Instrumentation Application and Design*, 5th ed. Wiley, Hoboken, 2020.

[18] J. Xu, S. Mitra, A. Matsumoto and S. Patki, "A wearable 8-Channel Active-Electrode EEG/ETI Acquisition System for Body Area Networks," in *IEEE J. of Solid-State Circuits*, vol. 49, no. 9, pp. 2005–2016, Sept. 2014. [Online]. Available: https://doi.org/10.1109/JSSC.2014.2325557.

[19] J. J. Halford, D. Sabau, F. W. Drislane, T. N. Tsuchida and S. R. Sinha, "American Clinical Neurophysiology Society Guideline 4: Recording Clinical EEG on Digital Media," *J. of Clin. Neurophysiology*, vol. 33, no. 4, pp. 317-319, Aug. 2016.

[20] American Clinical Neurophysiology Society, "Guideline Twelve: Guidelines for Long-Term Monitoring for Epilepsy," in *J. of Clin. Neurophysiology*, vol. 25, no. 3, pp. 170-180, June3, 2008. [Online] Available: https://www.acns.org/UserFiles/file/Guideline_Twelve__Guidelines_for_Long_Term.8.pdf.

[21] E. Niedermayer and F. Lopes Da Silva, "Electroencephalography: Basic Principles, Clinical Applications and Related Fields," Williams & Wilkins, 2005.

[22] R. F. Yazicioglu, P. Merken and C. V. Hoof, "Effect of electrode offset on the CMRR of the current balancing instrumentation amplifiers," in *Res. in Microelectronics and Electronics, 2005 PhD*, Dec. 2005.

[23] Z. Zhao, K. Ivanov, L. Lubich, O. M. Omisore, Z. Mei, N. Fu, J. Chen and L. Wang, "Signal Quality and Electrode-Skin Impedance Evaluation in the Context of Wearable Electroencephalographic Systems," in Proc. *IEEE Eng. Med. Bio. Conf. (EMBC)*, July 2018, pp. 4965-4968. 10.1109/EMBC.2018.8513457.

[24] A. Tautan, V. Mihajlovic, Y. Chen, B. Grundlehner, J. Penders, and W. Serdijn, "Signal quality in dry electrode EEG and the relation to skin electrode contact impedance magnitude" in *Biodevices*, 2014.

[25] L. Casal and G. L. Mura, "Skin-electrode impedance measurement during ECG acquisition: method's validation," in *J. of Phys.: Conf. Ser*, 705, 2016.

[26] M. Sheeraz, A. R. Rehman and M. A. B. Altaf, "Multiphysiological Shallow Neural Network-Based Mental Stress Detection System for Wearable Environment," Proc. *IEEE International Symposium on Circuits and Systems (ISCAS)*, May 2022, pp. 1-5.

[27] B. Taji, A. D. C. Chan and S. Shirmohammadi, "Effect of Pressure on Skin-Electrode Impedance in Wearable Biomedical Measurement Devices," in *IEEE Trans. Instrum. and Meas. (TIM)*, vol. 67, no. 8, pp. 1900-1912, Mar. 2018.